




RESEARCH ARTICLE

Simulation of overflow thresholds in urban basins: Case study in Tuxtla Gutiérrez, Mexico

Moisés Silva Cervantes^{1,2}  | Ana Hernando^{2,3} | Antonio García-Abril² |
Rubén Valbuena⁴ | Javier Velázquez Saornil³  | José Antonio Manzanera² 

¹Centro de Estudios para el Desarrollo Municipal y políticas Públicas, Universidad Autónoma de Chiapas, Tuxtla Gutiérrez, Mexico

²Research Group SILVANET, Universidad Politécnica de Madrid, E.T.S.I. Montes, Ciudad Universitaria, Madrid, Spain

³Research Group TEMSUS, Catholic University of Ávila

⁴School of Natural Sciences, Bangor University, Bangor, UK

Correspondence

José Antonio Manzanera, Research Group SILVANET, Universidad Politécnica de Madrid, E.T.S.I. Montes, Ciudad Universitaria, 28040 Madrid, Spain.
Email: joseantonio.manzanera@upm.es

Abstract

The space–time dynamics and the effect of urban growth on territory transformation were simulated with *Iber* 2D to analyze flooding events in the lower basin of the Sabinal River, Mexico. We classified the main coverages and land uses of the study area. Soil roughness and water infiltration in the soil were evaluated. Both values were used as input data in a simulation model with *Iber* 2D to analyze and compare the levels of water height and maximum flood level area with different precipitation values in two reference years, 1986 and 2014. Residential use land cover increased considerably while tree, pasture and agricultural use covers decreased. Consequently, in 2014, precipitation of similar magnitude led to higher values of direct runoff, increasing water levels and therefore the risk of overflowing. The water levels and moments of river overflow provided feedback for flood-risk warning systems and tools to monitor basins lacking adequate infrastructure.

1 | INTRODUCTION

Flood hazards due to extreme hydrometeorological events have become a recurrent problem in tropical and subtropical regions of the world (Hurford, Maksimovic, & Leitao, 2010). Many regions have been exposed to particularly severe flooding over the course of the last few years, much of which is due to land-use change (DeFries & Eshleman, 2004; Owangi, Lannigan, & Simonovic, 2014; Stonestrom, Scanlon, & Zhang, 2009). Flooding in urban areas is a major natural hazard causing loss of life and damage to property and infrastructure (Sowmya, John, & Shrivasthava, 2015; Zope, Eldho, & Jothiprakash, 2017). In southeastern Mexico, where the country's highest rainfall is recorded, serious problems have arisen in several watersheds due to extreme rainfall (Centro Nacional de Prevención de Desastres, 2005).

For proper local and regional management and planning, current and potential land uses must be mapped, in addition to identifying the main and secondary river channels and delineating flood areas, among other actions (Roca & Davison, 2010; Silva, García, & Hernando, 2015; Zope et al., 2017). Modern remote sensing technologies and Geographic Information Systems (GIS) are very useful in characterizing territory and carrying out temporal analyses to show the evolution and changes in land

cover and uses (Adnan, Iqbal, Maltamo, & Valbuena, 2018; Benza, Weeks, Stow, Lopez-Carr, & Clarke, 2016; Hernando, Velazquez, Valbuena, Legrand, & Garcia-Abril, 2017; Sowmya et al., 2015; Zope et al., 2017). Hydrometeorological models, on the other hand, are used to analyze the effect of rainfall on surface runoff, lag time, water height, among others factors, at the basin scale (Dal-Ré, 2003). In addition, there are different calculation methods and software that greatly facilitate hydraulic or hydrological modelling. Some of these tools have been used: Hec-Ras (Larios, Torres, Quevedo, Martínez, & Salgado, 2015; Ruiz-Bellet, Castelltort, Balasch, & Tuset, 2017), Hec-Hms (Juárez, Ibáñez, Pérez, & Arellano, 2009; Ren et al., 2017), Infoworks 2D (Falter et al., 2013; Hurford et al., 2010; Mundo, 2012; Roca & Davison, 2010) and the permanent-flow simulation program of the Autonomous University of Mexico (Aragón, 2007). Recently, the possibilities of the *Iber* 2D model (open-source software) have been explored, which allows 2-dimensional hydraulic simulation and also has a hydrological module (Bladé et al., 2014a, 2014b). *Iber* is a numerical simulation model of turbulent flow in free sheet in a nonpermanent regime and of environmental processes in environmental hydraulics. It allows the following applications: analysis of river hydrodynamics, simulation of dam failure, calculation of sediment transport and tidal flow in estuaries, as well as

evaluation of floodable areas (Centro de Estudios y Experimentación de Obras Públicas [CEDEX], 2010, 2012; Rivera, 2017). As the Sabinal River is intermittent, concentrating a large flow in the rainy season and low flow in the dry season, in addition to having a very irregular bed with variable channel widths and depths, *Iber* is very suitable for simulation tests on this river.

Although *Iber* was developed primarily for 2D hydraulic simulation (Garrote, Alvarenga, & Díez-Herrero, 2016), a hydrological module has been incorporated in its intermediate versions, which allows a good level of precision to represent rainfall-runoff processes (Juárez et al., 2014). Using its hydrological variables and routines, it can also be used to predict river overflows based on certain precipitation levels and terrain characteristics (Alvarez, Puertas, Pena, & Bermudez, 2017). The simulation models, when duly calibrated and validated, are used to reproduce rain events and, from them, generate forecasts of water levels, flows and runoff volumes (Ricardi et al., 2013). Hydrometeorological simulation can be performed in aggregate form or following a distributed pattern of input variables and results, that is, cell by cell of the digital terrain model (DTM) (Dal-Ré, 2003; Ricardi et al., 2013; Vélez, 2013). A distributed assignment of variables and certain parameters is possible with *Iber*, and results are obtained for each element of the terrain, rendering a semidistributed simulation model.

In recent decades, the Sabinal River has overflowed multiple times, mainly affecting the population of Tuxtla Gutiérrez, Chiapas, Mexico (Comisión Nacional del Agua [CONAGUA], 2004). Since October 2003, the Hydrometeorological Alert System for Tuxtla Gutiérrez (SAHT) was implemented (Salas, Jiménez, Eslava, Franco, & González, 2004) and several structural proposals have been built to reduce the risk of flooding inside this city (Aguilar, Domínguez, Guitchard, & Muciño, 2012). Using *Iber*, multiple applications were carried out to analyze areas of floodability (Soler, Bladé, Bofill, & Gamazo, 2013). In a conventional floodability study, first, the surface runoff generated by a given precipitation is calculated, and the hydraulic behaviour in the channels is then analyzed, estimating the height of the water sheets, speed and transfer times (Kaffas, Hrisanthou, & Sebastas, 2018; Vélez, 2013). Finally, a validation should be done by comparing simulated flows with known flow values. The problem is that true records are not always available. In our case, there were no actual values of recent flows recorded in the Sabinal River, but SAHT reference values on the water heights in the river were available, which prompted us to estimate the heights in the water sheets directly from precipitation values.

This article discusses the results of simulation tests with *Iber*, using detailed information of the topography and land cover, which were applied on a polygon from the Tuxtla Gutiérrez urban area, in order to address the following principal objective: to analyze how changes in land cover of the Sabinal River Basin have affected the values of water height reached following a given precipitation. It should be noted that this work is not intended to quantify the flows, or the water volume generated by precipitation, as in a classic hydrological-hydraulic study. Our focus is on the analysis of water heights reached within the main riverbed, in order to compare the risk

of overflowing in conditions with greater and lesser degrees of anthropization of the territory.

2 | MATERIAL AND METHODS

2.1 | Study area

The Sabinal River Basin, with a total area of 407 km², is located in Chiapas, Mexico, covering part of the municipalities of Tuxtla Gutierrez (state capital), San Fernando, Berriozabal and a small portion of Ocozacoautla. The altitude of the basin varies between 379 and 1,200 m, and following that altitude gradient, average annual temperatures are between 28°C at the lowest altitude and 20°C at the highest altitude, and average annual rainfall between 900 mm at the lowest altitude and 2,000 mm at the highest altitude (Secretaría de Hacienda, Gobierno Estatal de Chiapas, [SHGEC], 2014). The Sabinal River originates in Berriozabal, crosses the Tuxtla Gutiérrez Valley and flows into the Grijalva River. On its way, it collects the runoff from 15 main streams so that in the rainy season (May to October) its main channel can support up to 50 m³/s without overflow (Aragón, 2007; Gordillo & Castillo, 2017). The specific study area where the simulation tests were applied, concerns a 60 km² polygon in the lower part of the Sabinal River Basin, towards where all the streams in the basin drain. This polygon is located in the urban and densely populated area of Tuxtla Gutiérrez, from an elevation of 615 m in the west of the city, just where the river enters the city and crossing towards the east, to an elevation of 379 m, where it flows into the Grijalva River. The length of the main channel is 21.25 km, and the average slope is 1.12% (Figure 1).

Although this study area has a low average slope (1.2%), it is surrounded by steep slopes to the north and south, so rain tends to run off from north to south and from south to north until it reaches the main channel. The construction of housing developments and shops and the paving of streets in the central parts of the basin cause water to flow down streams and avenues, carrying sediment and residues that are deposited on plains or end up in the main channel. In October 2003, Tropical Storm Larry hit the Pacific coast of Mexico, causing damage to the Sabinal River Basin. Flooding of the river at various points affected 39,000 displaced inhabitants and some 49,700 houses, in addition to causing considerable damage to urban infrastructure and large numbers of businesses (CONAGUA, 2004). In 24 hr, maximum historical precipitation values of 131 mm in San Fernando and 225 mm in Berriozabal were recorded, generating an estimated flood of more than 300 m³/s in the Sabinal River (Mundo, 2012; UNO, Organización de las Naciones Unidas, 2010).

2.2 | Tuxtla Gutiérrez Hydrometeorological alert system (SAHT)

In order to monitor the precipitation and flows generated in the Sabinal Basin, the SAHT was installed in 2004, with seven rainfall

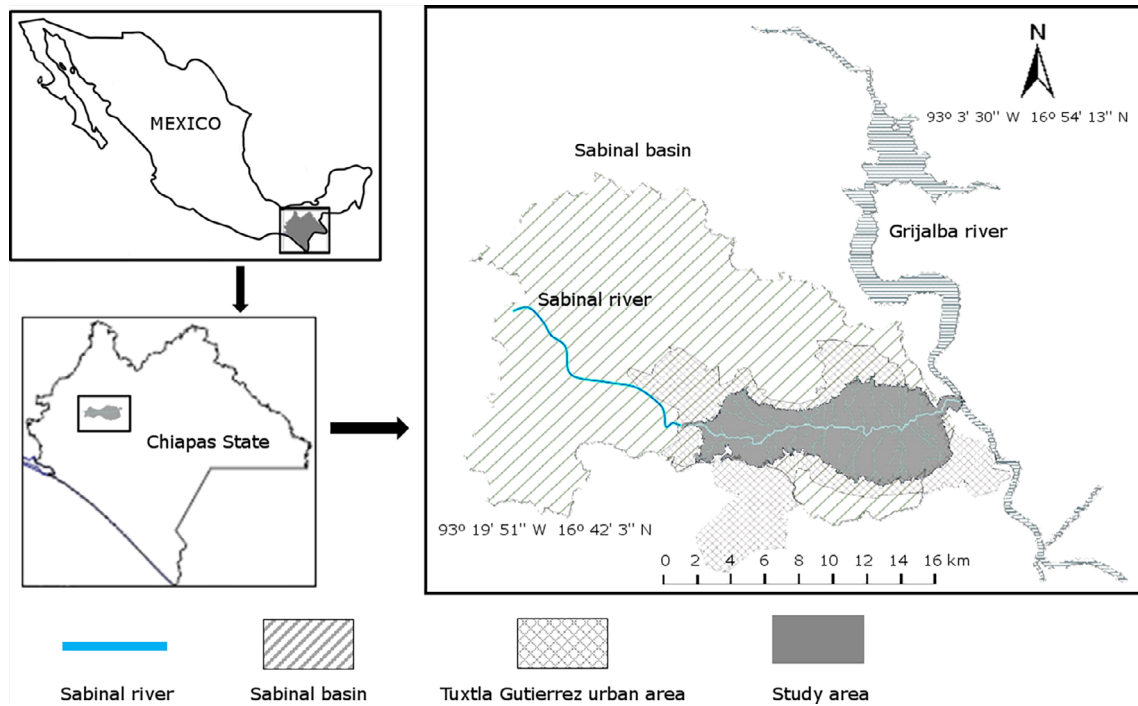


FIGURE 1 Study area, Chiapas state, Mexico. Data from Instituto Nacional de Estadística Geografía e Informática (INEGI, 2015b) and SHGEC (2014)

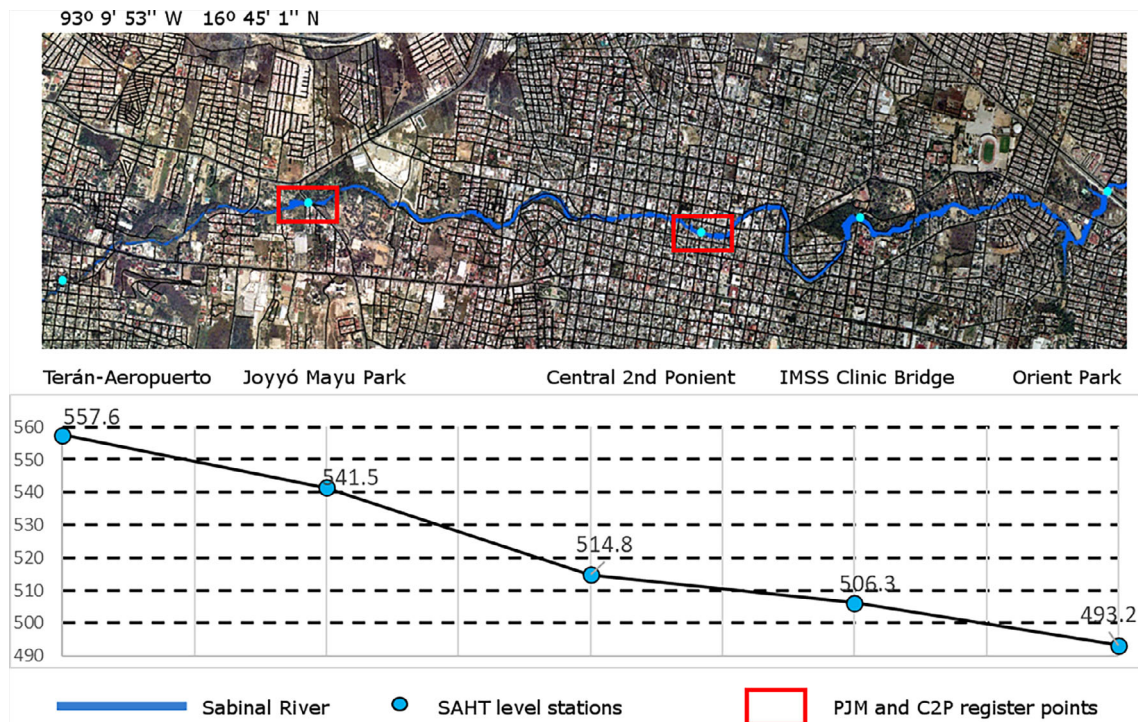


FIGURE 2 Tuxtla Gutiérrez hydrometeorological alert system level stations selected for *Iber* simulations (CONAGUA). Elevations in m

stations distributed in the middle and upper parts of the basin, and three level stations to record the height of the main riverbed as it passes under the bridges of Terán-Airport, Joyyó Mayú Park and Oriente

Park (Salas et al., 2004). Subsequently, with the creation of the Tuxtla Gutiérrez Hydrometeorological Center (CHT), dependent on the National Water Commission (CONAGUA), the equipment was

expanded with four new level stations, also located on bridges over the main channel of the Sabinal: Club Campestre (CC), Casa Kolping (KH), Centro 2 Poniente (C2P), and IMSS Clinic Bridge. All the level stations and three of the pluviometry stations are located within the study area (Figure 2).

Based on the riverbed height records, CONAGUA (2018) established the minimum, critical and maximum levels of each station, which allow monitoring and, where appropriate, alert the population about the risk of river overflow: (a) the minimum level corresponds to the height of the river bottom, (b) the critical level (approximately 60% height) indicates that there is a high risk of the river overflowing, and (c) the maximum level (100% height) corresponds to the height where the river definition is lost due to flooding (CONAGUA, 2004, 2018) (Table 1 and Figure 2). Based on the evidence gathered by the CHT, although the river drains very quickly, with 60 mm/hr precipitation over the city, the water levels increase significantly and the alert is activated since there is a risk of overflow in some points of the main channel; with 90 mm/hr or more, the river reaches its maximum level and overflows, which occurs mainly in two points: at Tuctlán Park (land elevation 542 m) and between the Street second Poniente and the Central Street (land elevation 514 m).

In this article, we compared the minimal, critical and maximum levels obtained through the simulation tests in five selected level stations (Table 1), which are distributed homogeneously along the main river channel, and correspond to points where overflows of the river have occurred (CONAGUA, 2004).

2.3 | Analysis of changes in land cover and land use

The land cover was obtained through supervised maximum likelihood classification of Landsat images (30 × 30 m optical bands), one from 1986 (Landsat 5 TM) and another from 2014 (Landsat 8 OTIS). We identified and quantified the coverage of (a) forest, (b) agricultural (grassland and crop fields), (c) bare ground, and (d) residential (housing developments and infrastructure). A confusion matrix was prepared,

TABLE 1 Level stations of the Tuxtla Gutiérrez hydrometeorological alert system (CONAGUA, 2004)

Level station	Water elevation (m)		
	Minimal ^a	Critical ^b	Maximum ^c
Terán-Aeropuerto	557.6	561.0	561.7
Parque Joyyó Mayu	541.5	544.7	546.0
Centro 2a. Poniente	514.8	518.1	519.2
Puente IMSS	506.3	509.5	511.5
Parque Oriente	493.2	497.0	499.0

^aMinimal: height of the river bottom.

^bCritical: 60% of the water elevation; there is a high risk of the river overflowing.

^cMaximum: 100% of the water elevation; the height at which river definition is lost due to the flooding.

and the Kappa index was calculated, obtaining an overall reliability of 80 and 85% in the 1986 and 2014 classifications, respectively. Based on this, the coverage A of 1986, and the coverage B of 2014 were obtained. The information obtained on the land cover was used to define distributed values of soil roughness (Manning coefficient, n ; Table 2), assuming the ranges proposed by Martínez and Fernández (2012). Also, an aggregate index of study area losses was obtained, weighting the Curve Number (Dal-Ré, 2003) with the corresponding proportions of each cover type (Table 3). The Curve Number Method (CN), developed by the Soil Conservation Service of the US Department of Agriculture (USDA SCS), is summarized in a set of values in tables used to estimate surface runoff from the physical and geomorphological characteristics of the basin and the types and uses of soil and vegetation (Dal-Ré, 2003; Martínez, 2001).

2.4 | Simulation of water height levels using Iber

First, a DTM was generated from Light Detection And Ranging (LIDAR) data, with pixel size 5 × 5 m and altitude resolution of 1.00 m, facilitated by the National Institute of Geography, Statistics and Informatics (INEGI, 2015a), which is the most accurate topographic information available in the region. The flight took place in 2007. The DTM was cleaned by removing bridges, buildings and trees from the riverbed or the flood zone with the intention of being able to model in a natural flow regime. However, each pixel retained the previous values of roughness and loss. Then, on an unstructured triangular mesh generated from the DTM by means of the RTIN method, simulation tests were performed with *Iber* version 2.3.4 software to observe the effect of rainfall as a function of land cover, for both 1986 and 2014 (Figure 3).

Iber operates on an unstructured mesh of finite volumes formed by triangular or quadrilateral elements. On each of the elements of the mesh, *Iber* performs calculations based on the equations of Saint-Venant 2D of finite volumes (Equation (1), and generates as results maximum values of flow rate, flow speed, depth and water level, among others.

For shallow water, in a horizontal bed, with no Coriolis forces, no wall friction or viscous forces, and no significant wind forces, the Saint-Venant 2D equations are simplified (López, Alavez, & Hernández, 2009; Rivera, 2017):

$$\frac{\partial h}{\partial t} + \frac{hu}{\partial x} + \frac{hv}{\partial y} = 0, \quad (1)$$

$$\frac{\partial}{\partial t}(hu) + u\frac{\partial}{\partial x}(hu^2 + gh^2/2) + \frac{\partial}{\partial y}(huv) = gh(S_{0y} - S_{0x}), \quad (2)$$

$$\frac{\partial}{\partial t}(hv) + \frac{\partial}{\partial x}(huv) + \frac{\partial}{\partial y}(hv^2 + gh^2/2) = gh(S_{0y} - S_{0x}), \quad (3)$$

where h is the depth; u and v are the components of the velocity vector in the directions x and y respectively; g is the acceleration of gravity; $S_{0x} = -\partial z/\partial x$ and $S_{0y} = -\partial z/\partial y$ measure the slope of the terrain in

TABLE 2 Default settings for the simulation tests with *Iber*. tr_1 ; $tr_{1.4}$; tr_{10} : return times

	Land coverage ^a		Roughness (mannings) ^b
	Coverage A: 1986	Coverage B: 2014	
1 Trees	5.95	7.18	0.12
Agricultural	40.38	21.4	0.04
Bare ground	0.34	1.66	0.15
Residential	13.65	30.08	0.023
Total	60.31	60.31	
	P1	P2	P3
Precipitation rate (mm/h) ^c	45 tr_1	60 $tr_{1.4}$	98 tr_{10}

^aLand cover areas obtained from Landsat image classification (km²).^bRoughness values proposed by Martínez & Fernández (2012).^cPrecipitation values were estimated for the indicated return times (tr) from the data series in Table 4.**TABLE 3** Weighted values of the Curve Number (CN) by cover type (1: Trees; 2: Agricultural crops; 3: Bare ground; 4: Residential) and year of satellite coverage (1986, 2014)

Cover type	CN	Coverage A: 1986	Weighted CN	Coverage B: 2014	Weighted CN
1 Trees	73	10%	7	12%	9
Agricultural	82	67%	55	35%	29
Bare ground	91	1%	1	3%	3
Residential	98	23%	22	50%	49
CN aggregate of the study area			85		89

Source: Prepared by the authors, based on Dal-Ré, 2003.

the directions x and y respectively; and z is a function that describes the channel bed.

The triangle mesh ranged from 5 to up 250 m, with 5 m for areas of highly irregular topography and up to 250 m for homogeneous areas (Figure 4). The mesh generated for the study area therefore comprised a total of 838,053 triangles. The mesh was very close to the real topography, providing reliable heights of depth and water levels. As can be seen in Figure 4, large triangles (up to 250 m size) were built up on areas with practically no slope, plains, floodplains, and wide streets and avenues of Tuxtla Gutiérrez. On the other hand, small triangles (5 m size) were built up on areas with steeper slopes, as occurs on the edges and bed of both the main channel and the streams of the Sabinal River. It was no use to define smaller areas because the maximum precision was limited by the DTM horizontal resolution (5 m-pixel), and a greater number of triangles would unnecessarily increase the processing duration.

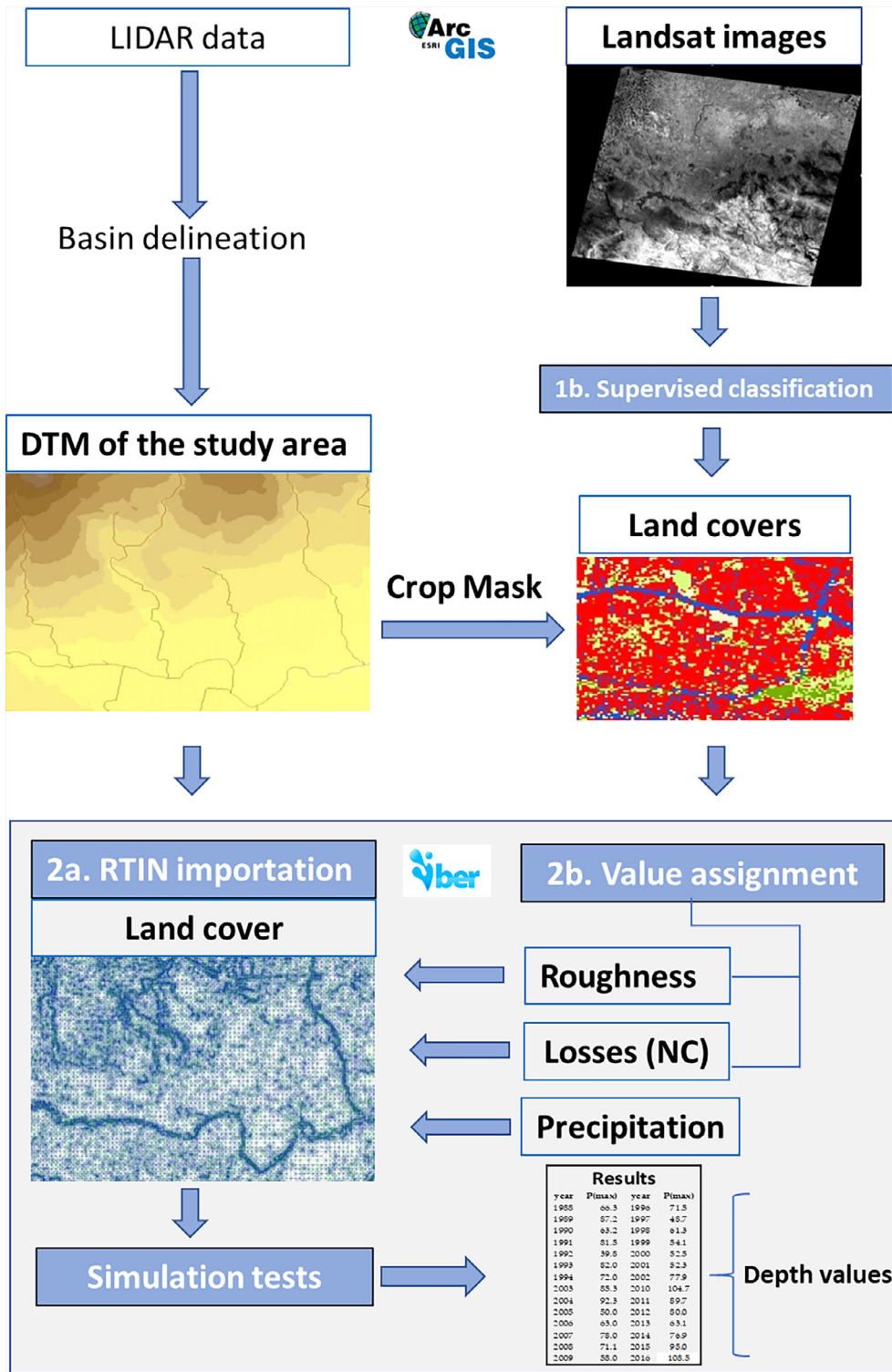
We performed a total of six simulation tests to observe the effect of rainfall as a function of land cover, for both 1986 and 2014 coverages, resulting from the combination of two coverage areas (Coverage A: 1986; Coverage B: 2014) and three precipitation levels (level p45: 45 mm/h; level p60: 60 mm/hr; level p98: 98 mm/hr). Each of the coverage areas was assigned a strong precipitation of 45 mm/hr (p45), which in theory does not exceed the capacity of the main channel of the Sabinal (Tests A1 and B1); subsequently, a very strong precipitation of 60 mm/hr (p60), which can cause overflowing in some

points of the river (tests A2 and B2); and, finally, an intense precipitation of 98 mm/hr (p98), which does cause overflowing of the river at several points, according to CONAGUA and National Meteorological Service's (SMN).

The 98 mm/hr value corresponds to a maximum rainfall in 24 hr (P_{max24}), for a 10-year return period (tr_{10} ; Table 2). Similarly, precipitations of 60 and 45 mm/hr correspond to return periods of 1.4 and 1 year, respectively (Table 2), for the same set of data. They were assigned to compare different levels of water height in the river, and to corroborate the values reported by CONAGUA. All of them were obtained by two different methods: the Gumbel method (Dal-Ré, 2003) and the log-Pearson Type III method (Bedient & Wayne, 2002), the standard technique used by Federal Agencies in the United States.

According to the Gumbel method, the maximum precipitation for a certain return period (P_{max24}) was calculated from a series of continuous historical data of the maximum annual precipitation in 24 hr. First, the standard deviation (S_x) and the average (\bar{Y}) were calculated from the historical data; then the values of the average of n years (Y_n) and the standard deviation of n years (S_n) were extracted from the Gumbel values (Table 4). Therefore, P_{max24} for each return period ($tr = 1, 1.4$ or 10 years, respectively; Table 2) was calculated by Equation (4):

$$P_{max24} = -\text{Ln}(-\text{Ln}(F(x)) * \alpha + \mu), \quad (4)$$



where $F(x) = 1 - (P > x)$; $P > x = tr^{-1}$; $\alpha = Sx/Sn$; and $\mu = \bar{Y} - (Yn * \alpha)$.

Table 4 shows the record of maximum annual rainfall values of 24 hr in pluviometer station No. 7202 from Tuxtla Gutiérrez, provided by the SMN, for the 1988–2016 period.

The Log-Pearson III (LPIII) method was also applied to corroborate the return periods corresponding to the selected rainfall, 45, 60 and 98 mm/hr. According to this method, the LPIII distribution is calculated using the following general equation:

$$\log X_{tr} = \overline{\log X} + KCs, tr * \sigma_{\log X}, \quad (5)$$

where X_{tr} is the precipitation value for a given return period (tr), $\overline{\log X}$ is the average of the log-precipitation values, factor K is a function of the skewness coefficient (Cs) and return period (tr) obtained from the K -value table for Gamma and log-Pearson Type III distributions, and $\sigma_{\log X}$ is the standard deviation of the $\log X$ values. As part of the method, operating with the historical precipitation values (Table 4) to arrive at the general

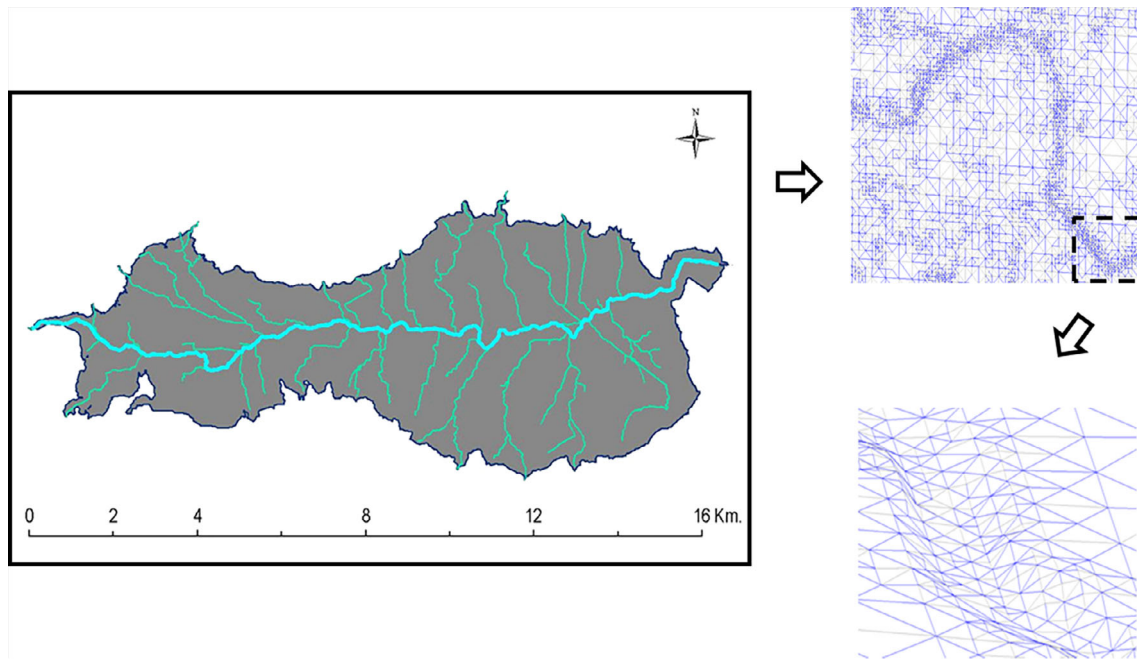


FIGURE 4 Section of Iber's unstructured and nonhomogeneous simulation mesh, in a stretch of the Sabinal River: the small triangles (equivalent to a minimum of 5 m) correspond to an irregular topography, typically near the river; large triangles (up to 250 m size) correspond to homogeneous topography

TABLE 4 Annual maximum 24-hr precipitation (data from the Hydrometeorological Station 7,202, Tuxtla Gutiérrez Chiapas, for the 1988–2016 period, CICESE, 2017)

Year	P(max)	Year	P(max)	Year	P(max)	Year	P(max)
1988	66.3	1996	71.5	2003	85.3	2010	104.7
1989	87.2	1997	48.7	2004	92.3	2011	89.7
1990	63.2	1998	61.3	2005	50.0	2012	80.0
1991	81.5	1999	54.1	2006	63.0	2013	63.1
1992	39.8	2000	52.5	2007	78.0	2014	76.9
1993	82.0	2001	52.3	2008	71.1	2015	95.0
1994	72.0	2002	77.9	2009	58.0	2016	108.5
1995	77.7						

formula, the mean, the standard deviation and skewness coefficient (C_s) were calculated through the following intermediate calculations:

$$\overline{\log X} = \frac{\sum_{i=1}^n \log X_i}{n}, \quad (6)$$

$$\sigma_{\log X} = \sqrt{\left(\sum_{i=1}^n (\log X_i - \overline{\log X})^2 / n - 1 \right)}, \quad (7)$$

$$C_s = \frac{n \sum_{i=1}^n (\log X_i - \overline{\log X})^3}{(n-1)(n-2)(\sigma_{\log X})^3}. \quad (8)$$

By introducing the intermediate calculations (Equations [6]–[8]) into the general equation (Equation [5]), and clearing the logarithm,

we obtained the corresponding precipitation values for each return period: $P(\max)_{tr_1} = 43$ mm/hr; $P(\max)_{tr_{1.4}} = 58$ mm/hr; and $P(\max)_{tr_{10}} = 97$ mm/hr. As can be seen, the precipitation values obtained by the LPIII algorithm were quite similar to those obtained by the Gumbel method (45, 60 and 98 mm/hr, resp.). Therefore, we chose the precipitation values obtained by the Gumbel method for the simulation tests since they were slightly less favourable and corresponded well to values reported by CONAGUA for precipitation events occurred in recent years.

The proposed simulation model assumes that rain falls uniformly over the entire area and is transformed into surface runoff. In turn, an initial dry condition is assumed (draft = 0), and given the topographic conditions of the basin, only one supercritical/critical output was declared. Then, no entry or exit conditions were imposed (CEDEX, 2012; Rivera, 2017).

During the preprocess stage with *Iber*, aggregated parameters were assigned on the simulation mesh: (a) initial condition dry and (b) losses weighted value (CN); and discretized parameters: (c) soil cover of each year (A or B) and (d) soil roughness values, assigned according to the cover type. As the independent variable, a hyetogram of intensities was assigned that emulates rainfall of 2.5 hr (with $P_{max_{24}} = 45$; $P_{max_{24}} = 60$; or $P_{max_{24}} = 98$ mm/hr, as calculated by Equation (4) for 1, 1.4 or 10 year-return periods, resp.). Rainfall was assigned by the alternate block method, assigning a higher precipitation in the centre of the hyetogram. For each rainfall, the simulated time was divided into 30-minute blocks (Table 2). The flow exit was located just where the Sabinal drains into the Grijalva River. Finally, the simulation period was set to 20 hr, with time steps of 5 min.

In the postprocessing stage with *Iber*, triangle elements were identified on the simulation mesh which were closely located and with bottom elevations close to the elevation of the five selected stations. The Nash Sutcliffe test was applied to validate the DTM used for the simulation mesh (see below). These elements were referred to as registration points and were identified by the following acronyms: TA, PJM, C2P, IB, PO (Table 5).

From *Iber*'s results files, the maximum values of flow depth (dependent variable) corresponding to each of the recording points were recovered (Table 5) and totalled to the bottom elevation to obtain the respective values of maximum water elevation (Figure 5). Likewise, for registration points JMP and C2P, the flood areas corresponding to the maximum depth values were obtained (Figure 6).

2.5 | Validation of the simulation model

In conventional floodability studies, first the surface runoff generated by a given precipitation is calculated and then, the hydraulic behaviour in the channels is analyzed, estimating the height of the water sheet, speed and transfer times. Finally, validation is done by comparing simulated flows with known flow values. Regarding hydrometeorological variables, although there are complete historical series of rainfall recorded in the pluviometry stations located in the Sabinal Basin, there is no consistent record of hydrometric

variables. The precipitation data of the SMN therefore cannot be correlated directly with the water flow and height values reported by CONAGUA.

In order to validate the results of the simulation model, the total runoff generated by p45, p60 and p98 on 2014 coverage (B coverage) was calculated using the curve number method (CN) (Table 6). This runoff was then compared with the total runoff values obtained by simulation tests with *Iber*. Both results were contrasted using the Nash-Sutcliffe index (Table 7).

2.5.1 | Estimation of total runoff using simulation tests with *Iber* ($Q_{sim,i}$)

Through the application of three tests with *Iber*, called B1, B2 and B3, the following total runoff values were obtained: p45 = 902,133.05 m³; p60 = 1,727,025.07 m³; and p98 = 3,684,071.36 m³.

2.5.2 | Estimation of total runoff using the CN method (qi)

Following the CN method, to estimate the surface runoff (Qm^3) produced by a determined precipitation (Pmm) from CN, first the potential retention (S , mm) is calculated:

$$S = 254 * (100/CN - 1). \quad (9)$$

Then, the direct runoff (Q , mm) generated by the precipitation (Pmm) is:

$$Q(mm) = \frac{(Pmm - 0.2 * S)^2}{Pmm + 0.8 * S}. \quad (10)$$

And finally, the total runoff (Qm^3) is calculated taking into account the entire basin area (A , m²):

$$Qm^3 = Q(mm) * 10^{-3} (m/mm) * A (m^2), \quad (11)$$

Following the CN method, Qm^3 also can be calculated both in distributed and aggregated forms, which can be done in a GIS through raster operations, as we did in this work (Table 6).

TABLE 5 Maximum depth values in the register points (m), based on the results of simulation tests with *Iber*

Register points	P1 = 45 mm/hr			P2 = 60 mm/hr			P2 = 98 mm/hr		
	A1: 1986	B1: 2014	Δ	A2: 1986	B2: 2014	Δ	A3: 1986	B3: 2014	Δ
TA	0.86	1.59	85%	1.87	2.49	33%	3.45	3.82	11%
PJM	0.99	2.17	119%	2.33	3.14	35%	4.03	4.47	11%
C2P	1.21	1.88	55%	2.61	3.03	16%	4.02	4.02	0%
IB	1.19	1.93	63%	2.26	2.90	28%	3.77	4.24	13%
PO	1.37	2.15	57%	2.76	2.98	8%	4.38	4.45	2%

Abbreviations: C2P, Centro 2 Poniente; IB, IMSS Clinic Bridge; PJM, Joyyó Mayú Park; PO, Oriente Park; TA, Terán-Airport; Δ, difference in water depth between 1986 and 2014 values, as percentage.

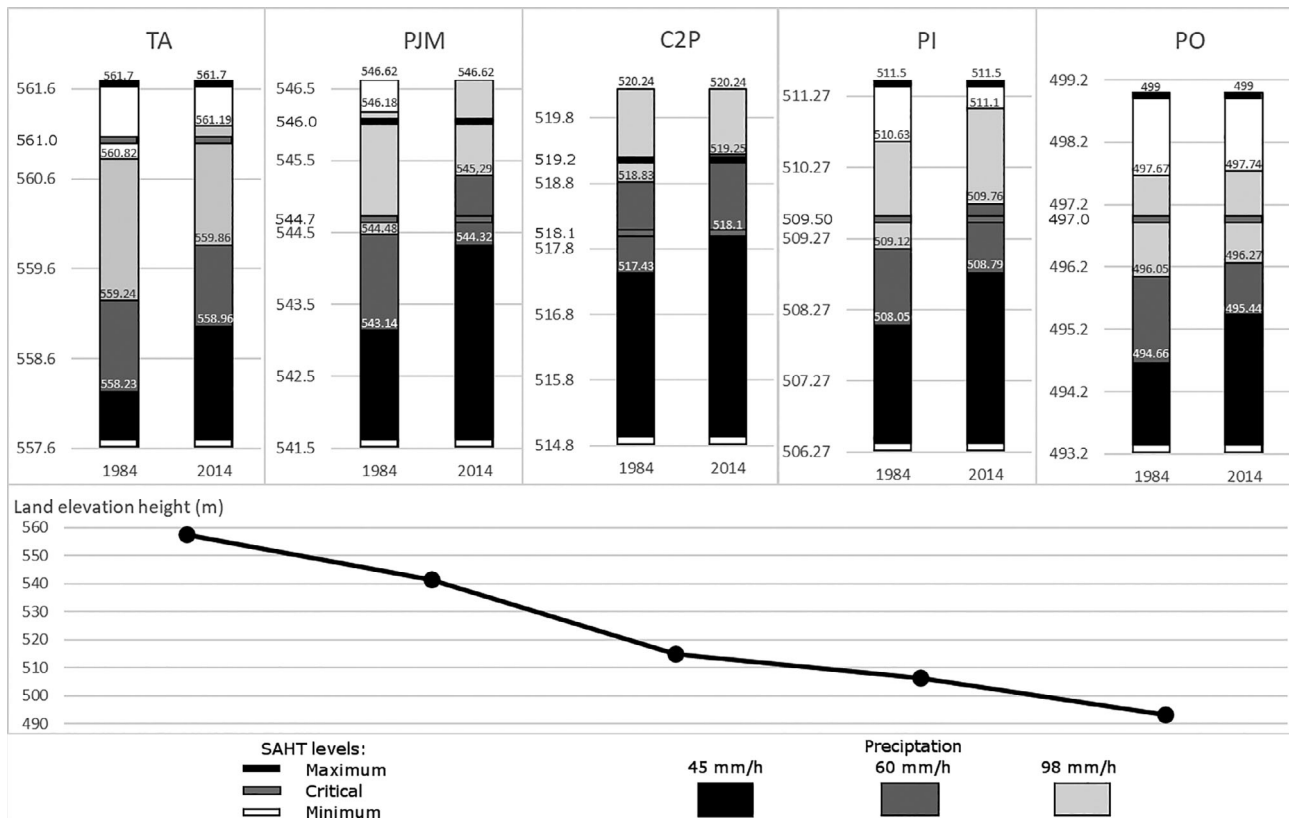


FIGURE 5 Water heights obtained at each registration point, in simulation tests with *Iber*. Source: Prepared by the authors, based on the results of simulation tests with *Iber*. Terán-Aeropuerto, Parque Joyyó Mayu, Centro 2 Poniente, PI and PO: level stations (see text)

2.5.3 | Nash-Sutcliffe criterion

The Nash-Sutcliffe index E compares simulated values ($Q_{sim,i}$) with actual values (Q_i). Depending on the value that E acquires, an evaluation criterion is issued on the fit of the model ($E < 0.2$ insufficient; $0.2-0.4$ satisfactory; $0.4-0.6$ good; $0.6-0.8$ very good; >0.8 excellent):

$$E = 1 - \frac{\sum (Q_{sim,i} - Q_i)^2}{\sum (Q_i - Q_{average})^2} \quad (12)$$

These simulated values with *Iber* ($Q_{sim,i}$) were contrasted by means of the Nash-Sutcliffe test (Equation [12]) with the estimated values by means of raster operations using the CN method (Equation [11]). Thus, for comparison purposes, we assumed as observed data (Q_i) those obtained by the CN method, given its generalized use. The test gave an $E = 0.78$ so we assumed that the fit between the results obtained with the model and those obtained using the CN method was very good (Table 7).

In addition, an empirical evaluation based on reports and evidence from CONAGUA on the occurrence of overflows in some points of the river was carried out, and the maximum water height values in the registration points were compared with the critical and maximum SAHT values.

In order to evaluate the quality of the DTM simulation grid, the Nash-Sutcliffe test was applied by comparing the river bed values reported in the SAHT (Q_i) with the bottom values corresponding to the

registration points identified in the simulation grid of *Iber* ($Q_{sim,i}$). In this case, the fit between the estimated grid values and the actual field values was excellent ($E = 0.99$), that is, the variations were minimal (Table 8).

3 | RESULTS

3.1 | Land cover change

The classification of the Landsat images from 1986 and 2014 showed a noticeable increase in urban cover in the municipality of Tuxtla Gutiérrez. The area for residential use and infrastructure increased annually by more than 3%, while the area for agricultural use (pastures and croplands) decreased by about 1% per year (Table 2). Tree cover remained almost constant over the 1986–2014 period, confined to parks and gardens as well as protected areas that have existed for several decades. However, outside the urban perimeter of Tuxtla Gutiérrez, in areas where there is no protection entity or sustainable management plan, tree and shrub cover has been replaced by residential or agricultural land. In both 1986 and 2014, there was no water cover in the study area, since the images correspond to the dry season when the streams are practically dry.

As a consequence of these land cover changes, the average values of roughness (n (1986) = 0.07; n (2014) = 0.11) and of losses (CN (1986) = 85; CN (2014) = 89) have changed, therefore altering the hydrological characteristics of the basin and the hydraulic response of the channels.

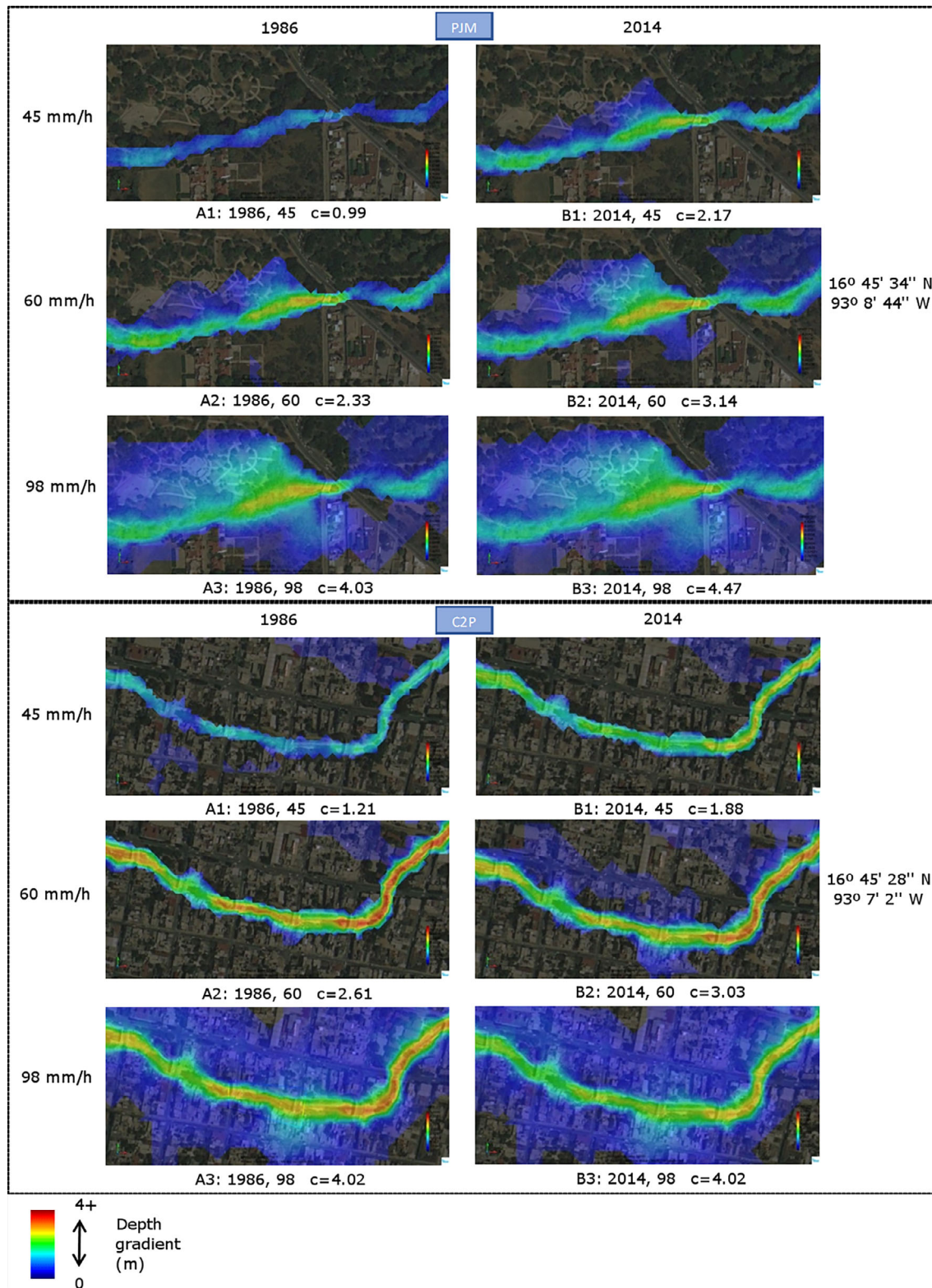


FIGURE 6 Depth values at the Parque Joyyó Mayu and Centro 2 Poniente registration points. Year A: 1986. Year B: 2014. Test 1:45 mm/hr; Test 2:60 mm/hr; Test 3:98 mm/hr. c: maximum depth (m)

3.2 | Effects of land cover change on depth values

Figure 5 illustrates the water behaviour at each of the registration points. The values of the minimum, critical and maximum levels of the

SAHT as well as the maximum water elevations obtained in the six simulation tests are shown and compared. It should be noted that each registration point has its own height scale, since the corresponding level stations are located at different land elevations

and also, the river channel varies in depth and width along its course. For example, the height of the TA station is 4.1 m, while JMP and C2P are 5.12 and 5.44 m, respectively, but in the latter two stations, the width of the channel is substantially reduced.

Although with p45 there is no overflow at any of the registration points in both years (Tests A1 and B1), the depth values are visibly larger in 2014 in comparison with 1986. The increases were 73, 118, 67, 74 and 78 cm at points TA, JMP, C2P, IB and OP, respectively. Therefore, the maximum water levels generated in 2014 with p45 (test B1) are considerably greater (55–119%). Although in no case the critical warning levels were exceeded with p45, in Test B1, the water level at C2P equalled the critical level, and at JMP it was very close to reaching it (Table 5 and Figure 5).

With p60, the critical level was exceeded only at C2P in 1986 (Test A2), but in 2014 (Test B2), the critical level was exceeded at JMP and IB, and even the maximum was surpassed at C2P. At the other register points, the values remained below their critical levels. The maximum depth values in simulation test B2 exceed those of test A2 at all stations, in a range of 8% (PO)–35% (PJM) (Table 5, Figure 5).

TABLE 6 Estimation of direct runoff by the CN method based on historical precipitation values and land cover of 2014 in Tuxtla Gutiérrez (coverage B)

	p = 45 mm	p = 60 mm	p = 98 mm
CN	92	92	92
S	22.09	22.09	22.09
Q (mm)	26.28	39.78	75.71
Q (m ³)	1,574,537.29	2,383,374.94	4,536,081.37
Area (A) (m ²)	59,913,900		

TABLE 7 Nash-Sutcliffe test: Validation of model results (Qm³)

P	Q _{sim,i}	Q _i
45 mm/hr	902,133.05	1,574,537.29
60 mm/hr	1,727,025.07	2,383,374.94
98 mm/hr	3,684,071.36	4,536,081.37
		E = 0.780727

Abbreviations: E, Nash-Sutcliffe value; Q_i, values estimated using the CN method (mm); Q_{sim,i}, values simulated with *Iber*, (mm).

TABLE 8 Nash-Sutcliffe test: Validation of minimum values of register points in simulation mesh (m)

Level station (SAHT)	Register points (mesh)	Q _{sim,i}	Q _i
Terán-Aeropuerto	TA	557.37	557.6
Parque Joyyó Mayu	PJM	542.15	541.5
Centro 2a. Poniente	C2P	516.22	514.8
Puente IMSS	IB	506.86	506.27
Parque Oriente	PO	493.29	493.2
			E = 0.999998

Abbreviations: E, Nash-Sutcliffe value; Q_i = river bed values in SAHT (mm); Q_{sim,i}, values simulated with *Iber*, (mm).

With p98, critical levels were exceeded in practically all the registration points for both years (A3 and B3 Tests), and maximum levels were exceeded at JMP and C2P; and with the coverage of 2014 (Test B3), the maximum level was almost reached at IB. Consequently, overflowing and flooding could be observed with p98 in the vicinity of points JMP and C2P (Figure 6). It should be noted that although the maximum levels were not reached at TA, IB and OP, with 98 mm in 2014 (Test B3), water levels close to such levels were reached (Table 5 and Figure 5).

The flood areas that appear at the JMP and C2P recording points, for the three precipitation values, 45, 60 and 98 mm/hr, and for the 2 years studied, 1986 and 2014, are shown in Figure 6. The flood areas increase as the precipitation value increases, and in general, they are greater in 2014 as compared to 1986. The flood areas obtained in the simulation tests at the JMP and C2P points coincide with the historical records of floods resulting from torrential rainfalls (CONAGUA). In the simulations with 1986 coverage, with p45 (Test A1) the water flows through the channel at both registration points; with p60 (Test A2) there is a moderate water height increase but the water remains within the channel; only with 98 mm rain (Test A3) does the water overflow and invade the floodplains. In the simulations with 2014 coverage, again, with p45 (Test B1) no flooding occurs; with p60 (Test B2) there is a slight overflow at C2P, along the southern river bank; and with p98, the overflow is generalized, encompassing housing areas in both PJM and C2P (Figure 6).

4 | DISCUSSION

The following can be inferred from the analysis of the classified images: The land cover changes between 1986 and 2014 altered the river basin's hydrological-hydraulic behaviour. The decrease in tree and shrub cover, as well as in bare soil and agricultural use, to expand land for residential and infrastructure use, increased the degree of waterproofing and, therefore, decreased the capacity of infiltration of water into the soil, at the same time that decreased the interception by vegetation. Consequently, the same precipitation regime generated greater surface runoff, greater flow volume and greater elevation of water in the main channel, thus increasing the risk of overflowing of the Sabinal River.

In addition to rapid urban growth, it should be noted that many of the new housing developments in Tuxtla Gutiérrez were located on

areas with steep slopes, especially in the northeastern zone of the city. Areas of natural runoff and flood plains, whose function consists precisely in naturally regulating flow excesses, were also invaded. In some cases, housing developments have been built-up within these spaces. Such actions have altered the river basin's hydrological balance and have increased the degree of vulnerability of the population in response to extreme hydrometeorological events (Palomeque et al., 2017; Zúñiga & Magaña, 2017). Given the topographical characteristics of the area and the alteration of its hydrological regime, a torrential rain on the city can cause overflowing of the river and flooding, even if there is a regulating dam upstream. Recurrently, as CONAGUA has documented, with intense rains, the river trends to overflow, mainly around JMP and C2P stations.

It is also important to note that water accumulates slightly around JMP and C2P stations as a result of runoff from elevated slopes, without causing any major problems; but when this is a result of Sabinal River overflows, depending on their magnitude, the population may be affected. The floodplain near the JMP station includes park areas and sports installations, while the use of the area near C2P is heavily residential, so an overflow will affect it much more (Figure 6).

The flow measurement points are necessary to ensure the representativeness of the spatial distribution of rainfall and runoff generated (Ricardi et al., 2013). At the same time, the timely recording and monitoring of flood flows and water height scales are fundamental for the operation of a hydrometeorological warning system (CONAGUA, 2004).

Typically, hydraulic simulation models are statistically validated by comparing the observed flow values (Q_i) with the simulated flows ($Q_{sim,i}$). In our case, given that we did not have Q_i values, we compared the validity of *Iber*'s numerical calculation method by contrasting the total runoff values ($Q_{sim,i}$) provided by *Iber*'s model with total runoff values calculated using the CN method (Q_i), finding a very good fit level. Also, we compared the effect of simulated precipitation with that of real precipitations, verifying that simulated and real floods occurred with similar precipitation thresholds. Therefore, we assume that the *Iber* simulation model yields satisfactory flow results and allows us to make good estimates of depths and maximum water height values in the river. The LIDAR-generated triangle mesh was adequate for hydraulic-hydrological simulation tests with *Iber*. The robustly calculated model warranted good results in the simulation tests of variables such as depth and flow rate, providing reliability in the prediction of rainfall-runoff-flood events and therefore risk of river overflow and delineation of flood zones.

In the simulation, we found that, as documented by CONAGUA, with rainfall greater than 90 mm, the Sabinal River overflows at some points, and with 60 mm, there is a high risk of river overflow. The results of the water elevations in the register points, obtained in the simulation tests with *Iber*, were consistent with the critical and maximum values corresponding level stations of SAHT and the simulated overflows occurred at the sites reported by CONAGUA, rendering a good representation of the actual water heights reached in the river with a given precipitation (Tables 1 and 5).

It is important to emphasize that a detailed DTM and good cartography of the land cover are essential to integrate a good simulation

model. The scale of the working files is very important in the hydraulic models if a good level of precision in the results is to be ensured. LIDAR is undoubtedly the best option to generate a robust DTM for later use in the hydraulic simulation (Soler et al., 2013). We were able to use a smaller pixel size than that used previously in other flood modelling studies on areas lacking accurate cartography due to budgetary constraints. For instance, a 30×30 m pixel size, with a vertical accuracy of ~ 10 m provided by the Shuttle Radar Topography Mission, was used in Mozambique (Alvarez et al., 2017), Pakistan (Adnan et al., 2018) and Ghana (Benza et al., 2016). On the other hand, the 5×5 m pixel size used here is similar to that used in other studies (Ruiz-Bellet et al., 2017). Furthermore, the LIDAR estimated vertical mean absolute error depends on the cover type, from ~ 20 cm for low grass, to ~ 1.2 m for shrubs (Hodgson, Jensen, Schmidt, Schill, & Davis, 2003). Smith, Edwards, Priestnall, and Bates (2006) estimated a vertical accuracy of ± 1 m for LIDAR DTM of 5 m spatial resolution. In our case and with similar spatial (5×5 m) and altitude (1 m) resolutions, the available LIDAR-generated DTM in the study area helped us to obtain good results in the hydraulic simulation: the values of bottom height (terrain elevation) at the registration points showed similar values to the corresponding minimum levels of the altitude stations reported by CONAGUA (Table 8). Therefore, the empirical and statistical validity of the proposed methodology was verified, confirming its usefulness for analyzing flood areas and comparing the effect of a given precipitation on different terrain conditions (Figure 3).

This methodology, while impractical for real-time monitoring of height levels, flows and total runoff volume, can serve two purposes: (a) as a tool for the configuration and feedback of hydrometeorological warning systems, and (b) to analyze risk of overflow and flooding in localities that lack infrastructure for real-time monitoring of water height levels, taking advantage of records from nearby rain seasons. There are a large number of rural basins, as well as small urban basins that do not have gauging sites or manual or automatic stations for recording water height levels. In these cases, the proposed methodology can be very useful since it does not require more extensive technical inputs or information.

The comparison between three rain events (45, 60 and 98 mm) with two land cover conditions (minor and major urbanization in 1986 and 2014, respectively) leads us to warn the urgency of applying effective control measures in urban planning. Priority should be given to environmental measures that, on the one hand, reduce the risk of the overflowing the Sabinal River and, on the other hand, restore ecological and landscape value of the region, such as tree cover, city gardens, restoration of wetlands, and recovery of banks and flood plains. However, if the trend towards increased waterproofing of the soil continues, a large investment will need to be made in urban infrastructure for the collection, control and conduction of rainwater, in addition to the environmental effects. In recent years, the rainwater drainage network has been replaced and expanded, which has improved the response of the urban basin to light-heavy rainfall events. Nevertheless, this network can be overwhelmed during extreme precipitation events, mainly due to the movement of sedimentary and residual material that can obstruct the sewage system, as well as the main channel, requiring cleaning and

unblocking. It is therefore important to analyze the response of natural watercourses independently, as has been attempted here.

5 | CONCLUSIONS

The main benefit of the analysis carried out here is to assist risk management authorities and stakeholders from urban areas where the availability of hydrological information is limited. Our methodology may be used to predict flood areas in case of atypical precipitation events, assess the population and infrastructures affected, design evacuation plans and foresee prevention measures. The increase in urban-residential land cover in Tuxtla Gutiérrez at the expense of tree, agricultural and grassland cover, has reduced the capacity for water infiltration in the soil and interception so that with extreme precipitation, the amount of run-off water is greater, which increases the risk of the overflowing the Sabinal River. Torrential rainfall, given the topographical characteristics of the study area and the high degree of impermeability induced, could result in an overflow, overriding the regulatory capacity of dams and water collectors located in the middle parts of the basin. In Tuxtla Gutiérrez, structural measures that reduce the risk of overflowing the Sabinal River and restore tree cover and other above-mentioned ecological and landscape measures should be encouraged. The proposed methodology can be used to compare the effect of certain precipitation thresholds on different land cover. A simulation model could also be useful to detect flood situations and water levels reached, depending on certain precipitation values, thus providing feedback to flood-risk warning systems. Such models may reproduce the basin behaviour even with limited resources. These models could therefore be a very useful tool to support small rural communities that lack infrastructure for real-time monitoring of water height levels and that do not have a flood risk map. Additionally, Remote Sensing and simulation models, coupled with GIS tools, have proven to be very valuable resources for the characterization of the territory and the analysis of flood events.

ACKNOWLEDGEMENTS

This work was supported by the Mexican Ministry of Public Education (Subsecretariat of higher Education) for Moises Silva Cervantes's PhD studies. This work was also supported by contracts at Universidad Politécnica de Madrid (UPM).

CONFLICT OF INTEREST

The authors declare no conflicts of interest.

DATA AVAILABILITY STATEMENT

The data that support the findings of this study are available from the corresponding author, [JA Manzanera], upon reasonable request.

ORCID

Moisés Silva Cervantes  <https://orcid.org/0000-0003-0411-6425>

Javier Velázquez Saornil  <https://orcid.org/0000-0002-9188-3827>

José Antonio Manzanera  <https://orcid.org/0000-0002-9058-071X>

REFERENCES

- Adnan, S., Iqbal, J., Maltamo, M., & Valbuena, R. (2018). Groundwater vulnerability assessment using GIS based DRASTIC model in district Peshawar, Pakistan. *Arabian Journal of Geosciences*, 11, 458. <https://doi.org/10.1007/s12517-018-3795-9>
- Aguilar, S. M., Domínguez M. R., Guitchard R. D. & Muciño P. J. (2012). Presa Rompepicos como alternativa de solución a las inundaciones provocadas por lluvias extremas en la ciudad de Tuxtla Gutiérrez, Chiapas. Paper presented at: XXII Congreso Nacional de Hidráulica. Aca-pulco, Guerrero, México.
- Alvarez, M., Puertas, J., Pena, E., & Bermudez, M. (2017). Two-dimensional dam-break flood analysis in data-scarce regions: The case study of Chipembe dam, Mozambique. *Water*, 9, 432. <https://doi.org/10.3390/w9060432>
- Aragón, H. J. (2007). Procesamiento hidráulico en un sistema de alerta hidrometeorológica y su aplicación al río Sabinal en Tuxtla Gutiérrez, Chiapas. (tesis doctoral). México D.F.: UNAM.
- Bedient, P. B., & Wayne, C. H. (2002). *Hydrology and floodplain analysis*. Upper Saddle River, NJ: Prentice-Hall, Inc.
- Benza, M., Weeks, J. R., Stow, D. A., Lopez-Carr, D., & Clarke, K. C. (2016). A pattern-based definition of urban context using remote sensing and GIS. *Remote Sensing of Environment*, 183, 250–264. <https://doi.org/10.1016/j.rse.2016.06.011>
- Bladé, E., Cea, L., Corestein, G., Escolano, E., Puertas, J., Vázquez-Cendón, M. E., ... Coll, A. (2014b). Iber: Herramienta de simulación numérica del flujo en ríos. *Revista Internacional de Métodos Numéricos Para Cálculo y Diseño en Ingeniería*, 30(1), 1–10. <https://doi.org/10.1016/j.rimni.2012.07.004>
- Bladé, E., Cea, L., Corestein, G., Escolano, E., Puertas, J., Vázquez-Cendón, M. E., & Luna, C. F. (2014a). Análisis de las inundaciones en la planicie tabasqueña 1995–2010. *Tecnología y Ciencias del Agua*, 5(3), 5–3.
- Centro de Estudios y Experimentación de Obras Públicas (CEDEX). (2010). *Iber: Manual de referencia hidráulico*. Madrid, Spain: CEDEX Retrieved from <http://iberaula.es/modelo-iber/descarga>
- Centro de Estudios y Experimentación de Obras Públicas (CEDEX). (2012). *Iber: Manual básico de usuario*. Madrid, Spain: CEDEX Retrieved from <http://iberaula.es/modelo-iber/descarga>
- Centro Nacional de Prevención de Desastres. (2005). Impacto socioeconómico de los principales desastres ocurridos en la república Mexicana en el año 2004. Mexico: Secretaría de Gobernación.
- Comisión Nacional del Agua (CONAGUA). (2004). Plan de Emergencia de Inundación del río Sabinal. México: CONAGUA. Retrieved from <http://proteccioncivil.chiapas.gob.mx/documentos/DOC02131109.pdf>
- Comisión Nacional del Agua (CONAGUA). (2018). Monitoreo y alertamiento de la Cuenca del Río Sabinal.
- Dal-Ré, T. R. (2003). *Pequeños Embalses de Uso Agrícola*. Madrid, Spain: Mundi-Prensa.
- DeFries, R., & Eshleman, N. K. (2004). Land-use change and hydrologic processes: A major focus for the future. *Hydrological Processes*, 18, 2183–2186. <https://doi.org/10.1002/hyp.5584>
- Falter, D., Vorogushyn, S., Lhomme, J., Apel, H., Gouldby, B., & Merz, B. (2013). Hydraulic model evaluation for large-scale flood risk assessments. *Hydrological Processes*, 27, 1331–1340. <https://doi.org/10.1002/hyp.9553>
- Garrote, J., Alvarenga, F. M., & Díez-Herrero, A. (2016). Quantification of flash flood economic risk using ultra-detailed stage-damage functions and 2-D hydraulic models. *Journal of Hydrology*, 541, 611–625. <https://doi.org/10.1016/j.jhydrol.2016.02.006>
- Gordillo, R. M., & Castillo, S. M. (2017). Cambio de uso del suelo en la cuenca del río Sabinal, Chiapas, México. *Ecosistemas y Recursos Agropecuarios*, 4(10), 39–49. <https://doi.org/10.19136/era.a4n10.803>
- Hernando, A., Velazquez, J., Valbuena, R., Legrand, M., & Garcia-Abril, A. (2017). Influence of the resolution of forest cover maps in evaluating fragmentation and connectivity to assess habitat conservation status. *Ecological Indicators*, 79, 295–302. <https://doi.org/10.1016/j.ecolind.2017.04.031>

- Hodgson, M. E., Jensen, J. R., Schmidt, L., Schill, S., & Davis, B. (2003). An evaluation of LIDAR- and IFSAR-derived digital elevation models in leaf-on conditions with USGS level 1 and level 2 DEMs. *Remote Sensing of Environment*, 84(2), 295–308.
- Hurford, A. P., Maksimovic, C., & Leitao, J. P. (2010). Urban pluvial flooding in Jakarta: Applying state-of-the-art technology in a data scarce environment. *Water Science and Technology*, 62, 2246–2255. <https://doi.org/10.2166/wst.2010.485>
- Instituto Nacional de Estadística Geografía e Informática (INEGI). (2015a). Mapa Digital de México. Retrieved from <http://www.inegi.gob.mx>
- Instituto Nacional de Estadística Geografía e Informática (INEGI). (2015b). México en cifras: Información nacional, por entidad federativa y municipios. Retrieved from <http://www.inegi.gob.mx>
- Juárez, D. J., Arganis, J. M., Domínguez, R., Esquivel, G. G., Bladé, E., Dolz, J., ... Corestein, G. (2014). Comparación del hidrograma de salida de una cuenca con un modelo hidráulico y un modelo distribuido, in: XXIII Congreso Nacional de Hidráulica. Resúmenes extendidos. Congreso Nacional de Hidráulica, Puerto Vallarta, Jalisco (México). Retrieved from https://www.iberaula.es/Temas/DisplayTema?id_tema=680
- Juárez, M. J., Ibáñez, C. L., Pérez, N. S., & Arellano, M. J. (2009). Uso del suelo y su efecto sobre los escurrimientos en la cuenca del río Huehuetán. *Ingeniería Agrícola y Biosistemas*, 1(2), 69–76.
- Kaffas, K., Hrissanthou, V., & Sebastas, S. (2018). Modeling hydro-morphological processes in a mountainous basin using a composite mathematical model and ArcSWAT. *Catena*, 162, 108–129.
- Larios, T. H., Torres, B. E., Quevedo, N. A., Martínez, M. M., & Salgado, T. J. (2015). Riesgo de inundación en la subcuenca del río La Antigua, Veracruz, México. *Tecnología y Ciencias del Agua*, 6(3), 39–56.
- López, L. J., Alavez, R. J., & Hernández, L. J. (2009). Solución numérica del modelo de Saint-Venant vía volúmenes finitos. *Revista de Ciencias Básicas UJAT*, 8(2), 34–53.
- Martínez, M. E. (2001). *Hidrología Práctica*. Madrid, Spain: Colegio de Ingenieros de Caminos, Canales y Puertos.
- Martínez, M. M., & Fernández R. D. (2012). Hidrología aplicada a las pequeñas obras hidráulicas. México D.F: COLPOS. Retrieved from http://www.sagarpa.gob.mx/desarrolloRural/noticias/2012/Documents/FICHAS%20TECNICAS%20E%20INSTRUCTIVOS%20NAVA/INSTRUCTIVO_HIDROLOG%C3%8DA.pdf
- Mundo, M. M. (2012). Algunas razones técnicas para no construir una presa en el río Sabinal en Tuxtla Gutiérrez, Chiapas. Paper presented at: XXII Congreso Nacional de Hidráulica. Acapulco, Guerrero, México.
- Owringi, A. M., Lannigan, R., & Simonovic, S. P. (2014). Interaction between land-use change, flooding and human health in metro Vancouver. *Canada Natural Hazards*, 72, 1219–1230. <https://doi.org/10.1007/s11069-014-1064-0>
- Palomeque, C. M., Galindo, A. A., Escalona, M. M., Ruiz, A. S., Sánchez, M. A., & Pérez, S. E. (2017). Análisis del cambio de uso del suelo en un ecosistema urbano en la zona de drenaje del río Grijalva, México. *Revista Chapingo Serie Ciencias Forestales y del Ambiente*, 23(1), 105–120. <https://doi.org/10.5154/r.rchscfa.2016.03.018>
- Ren, J. H., Zheng, X. Q., Chen, P., Zhao, X. H., Chen, Y. P., & Shen, Y. (2017). An investigation into sub-basin rainfall losses in different underlying surface conditions using HEC-HMS: A case study of a loess hilly region in Gedong Basin in the Western Shanxi Province of China. *Water*, 9, 870. <https://doi.org/10.3390/w9110870>
- Ricardi, G., Stenta, H., Scuderi, C., Basile, P., Zimmermann, E., & Trivisonno, F. (2013). Aplicación de un modelo hidrológico-hidráulico para el pronóstico de niveles de agua en tiempo real. *Tecnología y Ciencias del Agua*, 4(1), 83–105.
- Rivera, J.M.C. (2017). Recomendaciones técnicas de aplicación de modelos hidráulicos en cauces reales, Master's thesis, University of Seville.
- Roca, M., & Davison, M. (2010). Two dimensional model analysis of flash-flood processes: Application to the Boscastle event. *Journal of Flood Risk Management*, 3, 63–71. <https://doi.org/10.1111/j.1753-318X.2009.01055.x>
- Ruiz-Bellet, J. L., Castelltort, X., Balasch, J. C., & Tuset, J. (2017). Uncertainty of the peak flow reconstruction of the 1907 flood in the Ebro River in Xerta (NE Iberian Peninsula). *Journal of Hydrology*, 545, 339–354. <https://doi.org/10.1016/j.jhydrol.2016.12.041>
- Salas, S. M., Jiménez, E. M., Eslava, M. H., Franco, S. M., & González, P. J. (2004). Configuración del Sistema de alerta hidrometeorológica de la Ciudad de Tuxtla Gutiérrez, Chiapas. México: CENAPRED. Retrieved from http://www.cenapred.unam.mx/es/Transparencia/FAQ/SISI/Anexo8.2/04_17_DI_DM_RH_IH_20102004.pdf
- Secretaría de Hacienda del Gobierno del Estado de Chiapas (SHGEC). (2014). Perfiles Municipales de Chiapas 2010. Retrieved from <http://ceieg.chiapas.gob.mx/perfiles/>
- Silva, C. M., García, A. A., & Hernando, G. A. (2015). Crecimiento de la mancha urbana en la Zona Metropolitana de Tuxtla Gutiérrez (Chiapas, México). *Quehacer Científico en Chiapas*, 10(2), 35–41.
- Smith, M.J., Edwards, E.P., Priestnall, G., & Bates, P.D. (2006). Exploitation of new data types to create digital surface models for flood inundation Modeling; FRMRC Research Report UR3; FRMRC: University of Manchester, UK.
- Soler, G. L., Bladé, E., Bofill, A. J., & Gamazo, P. (2013). "Enfoque raster" del problema hidrodinámico del flujo en lámina libre en 2D. *Tecnología y Ciencias del Agua*, 4(4), 77–92.
- Sowmya, K., John, C. M., & Shrivastava, N. K. (2015). Urban flood vulnerability zoning of Cochin City, southwest coast of India, using remote sensing and GIS. *Natural Hazards*, 75, 1271–1286. <https://doi.org/10.1007/s11069-014-1372-4>
- Stonestrom, D. A., Scanlon, B. R., & Zhang, L. (2009). Introduction to special section on impacts of land use change on water resources. *Water Resources Research*, 45, W00a00. <https://doi.org/10.1029/2009wr007937>
- UNO, Organización de las Naciones Unidas. (2010). Adaptación al cambio climático y políticas públicas en el manejo del agua urbana en Tuxtla Gutiérrez, Chiapas. Tuxtla Gutiérrez, Chiapas: Fondo para el Logro de los Objetivos de Desarrollo del Milenio (ODM). Retrieved from http://www.cinu.mx/minisio/Programa_Conjunto_Agua/Memoria_Taller_Dialogo_TGZ.pdf
- Vélez, U. J. (2013). Estrategia de simulación hidrológica distribuida: integración conceptual de hidrología, hidráulica y geomorfología. *Revista Académica Colombiana de Ciencias*, 37(144), 393–409.
- Zope, P. E., Eldho, T. I., & Jothiprakash, V. (2017). Hydrological impacts of land use-land cover change and detention basins on urban flood hazard: A case study of Poisar River basin, Mumbai, India. *Natural Hazards*, 87, 1267–1283. <https://doi.org/10.1007/s11069-017-2816-4>
- Zúñiga, E., & Magaña, V. (2017). Vulnerability and risk to intense rainfall in Mexico: The effect of land use cover change. *Investigaciones Geográficas*, 95, 1–18. <https://doi.org/10.14350/ig.59465>

How to cite this article: Silva Cervantes M, Hernando A, García-Abril A, Valbuena R, Velázquez Saornil J, Manzanera JA. Simulation of overflow thresholds in urban basins: Case study in Tuxtla Gutiérrez, Mexico. *River Res Applic.* 2020;1–14. <https://doi.org/10.1002/rra.3642>